The Plant Cell, Vol. 16, 1378–1391, June 2004, www.plantcell.org

Proteomic Identification of Annexins, Calcium-Dependent Membrane Binding Proteins That Mediate Osmotic Stress and Abscisic Acid Signal Transduction in Arabidopsis

Sumin Lee,[1] Eun Jung Lee, Eun Ju Yang, Ji Eun Lee, Ae Ran Park, Won Hyun Song, and Ohkmae K. Park[2]

Kumho Life and Environmental Science Laboratory, Gwangju 500-712, Korea

Comparative proteomic analysis of the *Arabidopsis thaliana* root microsomal fraction was performed to identify novel components of salt stress signaling. Among the salt-responsive microsomal proteins, two spots that increased upon salt treatment on a two-dimensional gel were identified as the same protein, designated annexin 1 (AnnAt1). Annexins comprise a multigene family of Ca^{2+}-dependent membrane binding proteins and have been extensively studied in animal cells. AnnAt1 is strongly expressed in root but rarely in flower tissue. In this study, the results suggest that salt stress induces translocation from the cytosol to the membrane and potential turnover of existing protein. This process is blocked by EGTA treatment, implying that AnnAt1 functions in stress response are tightly associated with Ca^{2+}. T-DNA insertion mutants of *annAt1* and a different isoform, *annAt4*, displayed hypersensitivity to osmotic stress and abscisic acid (ABA) during germination and early seedling growth. The results collectively suggest that AnnAt1 and AnnAt4 play important roles in osmotic stress and ABA signaling in a Ca^{2+}-dependent manner.

INTRODUCTION

Soil salinity is one of the most significant abiotic stresses, especially for crop plants, leading to reductions in productivity. Salt stress causes accumulation of excess toxic Na^+, along with deficiency of K^+, and turgor changes in the cytosol, which in turn induce ionic and osmotic stress in plants, respectively. Salt-induced ionic stress is clearly distinct from other types of stress, whereas osmotic stress is generally induced by salt, cold, and drought. Plant cells have the capacity to adapt to stress conditions by triggering a network of signaling events.

Genetic analyses have led to the elucidation of the salt overly sensitive (SOS) signaling pathway that controls ionic stress responses (Wu et al., 1996; Liu and Zhu, 1997; Zhu et al., 1998). SOS3, a Ca^{2+} binding protein, senses the Ca^{2+} change elicited by salt stress (Quintero et al., 2002). The protein physically interacts with and activates SOS2, a Ser/Thr protein kinase, in a Ca^{2+}-dependent manner (Halfter et al., 2000). The SOS3-SOS2 kinase complex regulates the expression and transport activity of ion transporters such as SOS1, a plasma membrane Na^+/H^+ exchanger, eventually removing Na^+ from the cytosol (Qiu et al., 2002).

[1] Current address: Department of Molecular Biology, Sejong University, 98 Gunja-dong, Gwangjin-gu, Seoul 143-747, Korea.

[2] To whom correspondence should be addressed. E-mail omkim@kkpc.com; fax 82-62-972-5085.

The author responsible for distribution of materials integral to the findings presented in this article in accordance with the policy described in the Instructions for Authors (www.plantcell.org) is: Ohkmae K. Park (omkim@kkpc.com).

Article, publication date, and citation information can be found at www.plantcell.org/cgi/doi/10.1105/tpc.021683.

Evidence has been presented showing that the osmotic stress response is mediated by signaling pathways distinct from the SOS pathway, with the identification of several protein kinases activated by osmotic stress (Zhu, 2002). Mitogen-activated protein kinases (MAPKs) are activated by hyperosmotic stress (Xiong et al., 2002). Specific MAPKs, such as salt stress–inducible MAPK and salicylic acid–induced protein kinase, are present in alfalfa (*Medicago sativa*) and tobacco (*Nicotiana tabacum*) cells, respectively (Munnik et al., 1999; Mikolajczyk et al., 2000). In *Arabidopsis thaliana*, at least three MAPKs are activated by salt and other stresses (Ichimura et al., 2000; Droillard et al., 2002). Ca^{2+}-dependent protein kinases have also been implicated in the osmotic stress response in association with Ca^{2+} signaling (Romeis et al., 2001). The plant hormone abscisic acid (ABA) has long been known to play a critical role in stress responses (Giraudat et al., 1994; Himmelbach et al., 2003). Whereas osmotic and cold stresses induce increased levels of ABA (Zeevaart and Creelman, 1998), some osmotic stress–responsive genes are induced by ABA (Skriver and Mundy, 1990). In addition, phospholipid signaling is closely related to osmotic stress (Zhu, 2002). Osmotic stress, cold, and ABA activate phospholipases that generate the second messengers, inositol 1,4,5-trisphosphate, diacylglycerol, and phosphatidic acid, which act in signaling pathways implicated in stress resistance (Dove et al., 1997; Munnik et al., 2000; DeWald et al., 2001). ABA and phospholipid molecules appear to function upstream of the osmotic stress–activated protein kinases. In plants, different signaling processes are integrated to cope with osmotic stress.

ABA, cold, drought, and salt stress trigger elevations in the cytosolic Ca^{2+} level in plant cells (Knight et al., 1996; Knight and Knight, 2001). As a second messenger, Ca^{2+} activates signaling pathways and therefore influences multiple aspects of cellular

functions (Knight et al., 1996, 1997; Trewavas, 1999). Ca^{2+} binding proteins serve as transducers of the Ca^{2+} signal. Ca^{2+} binding proteins have been identified in plants, such as calmodulin (Zielinski, 1998; Luan et al., 2002), Ca^{2+}-dependent protein kinases (Harmon et al., 2000; Romeis et al., 2001), calcineurin B–like proteins (Luan et al., 2002), and SOS3 (Liu and Zhu, 1998). Certain of these proteins are involved in ABA and abiotic stress responses (Sheen, 1996; Sajio et al., 2000; Townely and Knight, 2002).

Despite considerable progress in understanding stress signal transduction, the mechanisms of stress response remain largely unknown (Xiong et al., 2002). The identification of novel signaling components should contribute to the clarification of stress signaling. After the completion of genome sequencing in Arabidopsis, the identification of stress-responsive proteins is currently feasible with proteomics. In this study, the microsomal proteome from Arabidopsis roots was isolated and analyzed using two-dimensional (2D) gel electrophoresis and matrix-assisted laser desorption/ionization time of flight mass spectrometry (MALDI-TOF MS). In an attempt to identify the membrane proteins involved in salt stress, we evaluated salt-induced changes in the microsomal proteome and identified Ca^{2+}-dependent membrane binding proteins, designated annexins, as the signaling components of the stress response. Two-dimensional gel analyses combined with protein gel blotting revealed that levels of annexin 1 (AnnAt1) significantly increase in the microsome in a Ca^{2+}-dependent manner in response to osmotic stress. The *annAt1* and *annAt4* mutant plants were hypersensitive to salt and ABA during seed germination and early seedling growth. Based on these findings, we propose that annexins comprise a novel class of Ca^{2+} binding proteins that play important roles in ABA-mediated stress response in plants.

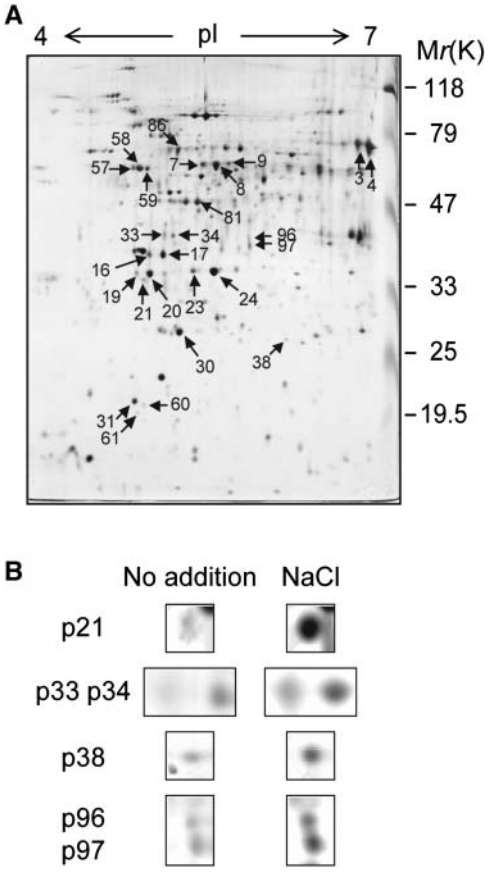

Figure 1. Two-Dimensional Gel Electrophoresis Analysis of Root Microsomal Proteins.

Root microsomal proteins were isolated from roots of 2-week-old seedlings grown in MS liquid media, separated by 2D gel electrophoresis, and visualized by silver staining.

(A) Microsomal proteins resolved in the range of pH 4 to 7. Protein spots identified by MALDI-TOF MS are numbered and listed in Table 1.

(B) NaCl-responsive microsomal proteins. Salt-responsive changes in protein expression were analyzed in gels prepared with the microsomal proteins from seedlings either untreated (left) or treated with 250 mM NaCl (right) in MS liquid media for 2 h. The spot numbers are the same as those specified in **(A)** and in Table 1.

RESULTS

Proteomic Identification of Salt Stress–Responsive Microsomal Proteins in Arabidopsis

To identify salt stress–regulated microsomal proteins, we conducted a comparative proteomic analysis. Microsomal proteins were isolated from roots of Arabidopsis seedlings either untreated or treated with 250 mM NaCl for 2 h and resolved by 2D gel electrophoresis. In this study, we focus on root tissue for many reasons. The root is the site of salt uptake; thus, the physiology of its salt response has been well characterized (Davies and Zhang, 1991; Kiegle et al., 2000). Moreover, the root is almost devoid of ribulose 1,5-bisphosphate carboxylase/oxygenase, the most abundant leaf protein, which limits protein loading on 2D gels and consequently prevents visualization of low-abundance proteins.

A 2D gel of root microsomal proteins revealed ~350 protein spots evenly distributed between pH 4 and 7 and molecular masses of 10 to 120 kD (Figure 1A). We randomly selected and identified spots with MALDI-TOF MS (Figure 1A, Table 1). The most prominent proteins were identified as mitochondrial and vacuolar ATPases. To analyze the salt response of root microsomal proteins, changes in spot intensity between untreated and treated samples were quantified by software analysis (see Methods). Protein spot changes were scored only when they were reproducibly observed in three independent experiments. Of the protein spots displaying greater than twofold upregulation or downregulation, six (spot numbers 21, 33, 34, 38, 96, and 97) were subjected to identification with MALDI-TOF MS analysis (Figure 1B, Table 1).

Among the salt-responsive proteins, p33 and p34 (spot numbers 33 and 34) representing AnnAt1 were initially selected for further characterization. AnnAt1 is an interesting molecule for several reasons. First, annexins participate in essential cellular processes in animal cells (Gerke and Moss, 2002). Second, their properties are directly regulated by Ca^{2+} that is implicated in stress response in plants (Knight et al., 1996; Knight and Knight,

Table 1. Identification of Root Microsomal Proteins in Arabidopsis Using MALDI-TOF MS

Spot No.[a]	Apparent MM (kD)/pI[b]	Match MM (kD)/pI[c]	MOWSE Score[d]	No. MP[e]	Percent Covered[f]	Accession No.[g]	Protein Name[h]
3	73.04/6.4	59.72/6.4	2.77E+09	20	43	15232626	Thioglucosidase 3D precursor
4	71.07/6.5	59.75/6.4	6.96E+04	13	30	1363489	Thioglucosidase 3D precursor
7	62.99/5.4	63.37/6.5	5407	7	19	1732570	Mitochondrial F1 ATP synthase β subunit
8	62.99/5.5	63.37/6.5	1.87E+13	24	47	1732570	Mitochondrial F1 ATP synthase β subunit
9	62.99/5.6	63.37/6.5	1.68E+08	14	31	1732570	Mitochondrial F1 ATP synthase β subunit
17	37.24/5.2	24.54/4.9	6058	7	34	21554133	Endomembrane-associated protein
19	34.64/5.0	41.86/5.4	7.87E+04	14	29	15222075	Actin 8
20	34.53/5.1	32.02/5.1	4288	8	29	15228216	Putative lectin
21	33.63/5.1	29.16/5.1	6.62E+04	7	35	21595512	Caffeoyl-CoA *O*-methyltransferase-like
23	34.87/5.4	32.16/5.5	8624	8	36	15228198	Putative lectin
24	34.76/5.5	32.12/5.5	5.57E+05	11	66	21594017	Putative lectin
30	26.45/5.3	28.17/5.7	7.24E+04	12	47	21536745	Ferritin 1 precursor
33	40.42/5.2	35.78/5.2	1.47E+06	11	44	1429207	Annexin
34	40.42/5.3	35.78/5.2	3.17E+10	19	68	1429207	Annexin
38	25.74/6.0	21.80/6.0	6.41E+06	7	47	15239652	1,4-Benzoquinone reductase-like; Trp repressor binding protein-like
57	61.29/5.0	54.74/5.0	7.51E+06	14	29	137465	Vacuolar ATP synthase subunit B
58	61.29/5.0	54.74/5.0	9.82E+07	15	34	137465	Vacuolar ATP synthase subunit B
59	61.29/5.1	54.74/5.0	3.47E+04	9	18	137465	Vacuolar ATP synthase subunit B
61	18.56/5.0	15.08/5.1	1.89E+06	9	63	15238776	Cytochrome b5
81	48.37/5.4	42.62/5.4	5.68E+06	12	33	18391442	Vacuolar ATP synthase subunit C, putative
86	70.30/5.3	55.33/5.2	9.36E+04	13	34	6685244	ATP synthase α chain
96	40.16/5.7	35.32/5.6	8.98E+04	9	36	1754983	Strictosidine synthase
97	38.86/5.7	35.32/5.6	1436	5	22	1754983	Strictosidine synthase

[a] Number of spot.
[b] Observed molecular mass (MM) and pI of spot from the gel.
[c] Predicted molecular mass (MM) and pI of matched sequence.
[d] Molecular weight search score.
[e] Number of peptides matching to predicted protein sequence.
[f] Percentage of predicted protein sequence covered by matched peptides.
[g] Accession number against the National Center for Biotechnology Information (NCBI) nonredundant database.
[h] Entry name according to the NCBI database.

2001). p33 and p34 protein spots migrated with a molecular mass of 40 kD, which is slightly larger than the theoretical molecular size of AnnAt1 (36 kD). The apparent pI values of p33 and p34 on a 2D gel are 5.2 and 5.3, consistent with the theoretical pI (5.2).

Expression of AnnAt1 in Tissues

To further characterize AnnAt1, we generated an antibody against an AnnAt1-specific peptide (amino acids 204 to 215). The specificity of the anti-AnnAt1 antibody was examined by protein gel blot analysis. The antibody specifically recognized recombinant AnnAt1 protein generated in *Escherichia coli* (data not shown), and a protein with a molecular mass of AnnAt1 and some higher molecular weight proteins in crude extracts prepared from tissues (Figure 2). In protein gel blot analysis of 2D gels, both p33 and p34 protein spots were detected by the anti-AnnAt1 antibody (Figure 3). However, additional protein spots with the slightly smaller size were also detected on 2D gels (Figure 3A). They are proportional to AnnAt1 protein in spot intensity and thus could be degraded forms of AnnAt1 protein, produced during the sampling process for 2D gel analysis. Based on the data, the anti-AnnAt1 antibody appears relatively specific under conditions tested.

The expression pattern of AnnAt1 in tissues was determined by protein gel blot analysis. AnnAt1 was expressed predominantly in root tissue (Figure 2). The immunodetectable level of AnnAt1 in roots from Arabidopsis grown in soil was similar to that in Arabidopsis roots cultured in MS media used throughout the experiments.

Expression of AnnAt1 Protein in Response to NaCl and Other Abiotic Stress

The salt response of AnnAt1 expression was further investigated by protein gel blotting. Two-dimensional gels prepared with root microsomal proteins were probed with the anti-AnnAt1 antibody. In a dose–response experiment, AnnAt1 protein was induced by treatment with NaCl at different concentrations. Proteins were most strongly induced at 250 mM NaCl (Figure 3B).

Next, we examined whether AnnAt1 expression is affected by ABA and other stress. We found that AnnAt1 protein was induced

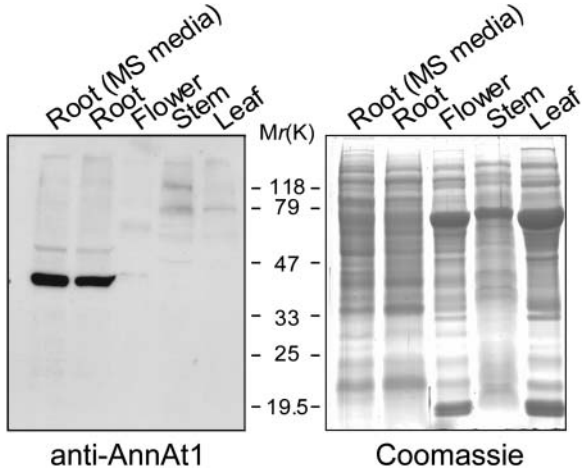

Figure 2. Expression of AnnAt1 in Tissues.

Crude extracts from various tissues were separated by SDS gel electrophoresis and subjected to Coomassie blue staining (right) and protein gel blot analysis with the anti-AnnAt1 antibody (left). Root (MS media) signifies roots grown in MS liquid media. Other tissues were prepared from 3-week-old plants grown in soil.

by ABA (Figure 3C). Treatment with mannitol and polyethylene glycol (PEG) additionally elevated AnnAt1 levels (Figure 3C), suggesting that the protein is sensitive to ABA and general osmotic stress.

Immunoblotting of 2D gels with the anti-AnnAt1 antibody revealed at least four spots, including p33 and p34 (Figures 3 and 4). Two additional 40-kD spots are unlikely to be other members of the annexin gene family that have the theoretical pI values between 5.8 and 9.5. To verify that the additional spots represent AnnAt1 protein, the spots were eluted from the gel and subjected to MALDI-TOF MS. Peptide masses from the spectra matched that of AnnAt1 in the database search, indicating that all four spots represent AnnAt1 protein (data not shown).

Subcellular Distribution of AnnAt1 Protein in Response to Salt Stress

The immunodetectable levels of AnnAt1 protein was examined in the microsomal and cytosolic fractions from Arabidopsis roots grown under normal conditions. AnnAt1 was detected in both the cytosol and microsome but was ~15-fold more abundant in the cytosol when estimated in the same amount of proteins (Figures 4A and 4E). Whether microsomal AnnAt1 is distinct from the cytosolic form with respect to function and structure remains to be elucidated.

We compared the salt-induced changes in AnnAt1 protein of the microsomal and cytosolic fractions by protein gel blot analysis of 2D gels. Immunodetectable AnnAt1 protein levels were considerably enhanced in the microsome after 2 h of salt treatment and fully recovered at 24 h (Figures 4A and 4E). Notably, the expression pattern was reversed in the cytosol, being almost completely abolished at 2 h of salt treatment and recovered thereafter. The pattern of expression of total AnnAt1 was similar to that of cytosolic AnnAt1, consistent with the fact that the cytosol constitutes the major fraction (>99%) and microsomes are very diluted (<1%) in the total fraction. The microsomal fraction was highly concentrated from the total fraction by ultracentrifugation. The results suggest that salt treatment affects AnnAt1 protein in two ways: specifically, translocation from the cytosol to the membrane and protein turnover in the cytosol.

The Ca^{2+} dependency of the subcellular distribution of AnnAt1 protein was examined. Plant extracts were incubated with either Ca^{2+} or EGTA before fractionation. Ca^{2+} increased the relative amount of AnnAt1 protein associated with the microsomal fraction, whereas EGTA had the opposite effect (Figure 4B). We further investigated the Ca^{2+} effect on salt response of AnnAt1 protein in vivo. The subcellular distribution of AnnAt1 protein was determined in Ca^{2+}-depleted plants incubated in MS media containing EGTA. Association with the membrane and Na^{+}-stimulated reduction in amount of AnnAt1 protein were both inhibited by EGTA (Figure 4C). AnnAt1 levels were partially affected, possibly because of incomplete Ca^{2+} chelation in

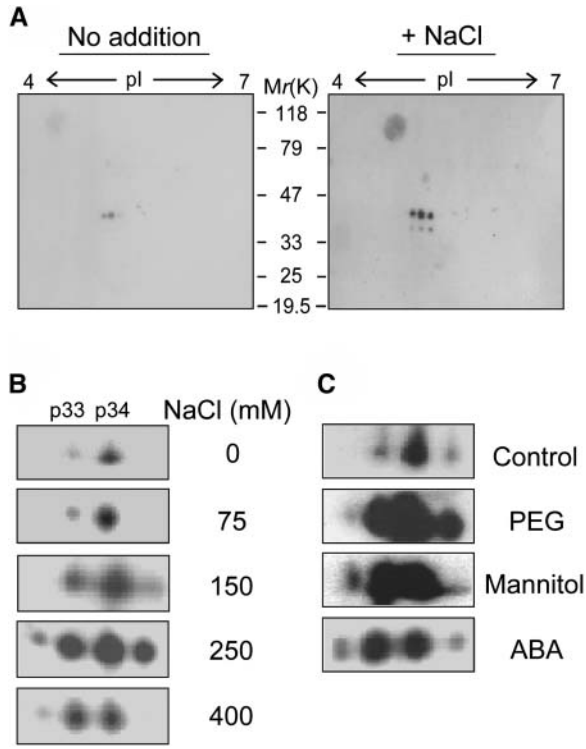

Figure 3. Expression of AnnAt1 in Response to Abiotic Stress.

Two-week-old seedlings grown in MS liquid media were incubated for 2 h at the specified conditions. Microsomal proteins prepared from root tissue were subjected to 2D gel electrophoresis and protein gel blotting with the anti-AnnAt1 antibody. Similar results were obtained in more than five independent experiments.

(A) AnnAt1 protein spots on the entire 2D gels. Two representative gels (0 and 250 mM NaCl) are shown.

(B) NaCl dose response of microsomal AnnAt1 protein.

(C) Treatment with 20% PEG, 0.25 M mannitol, and 100 μM ABA.

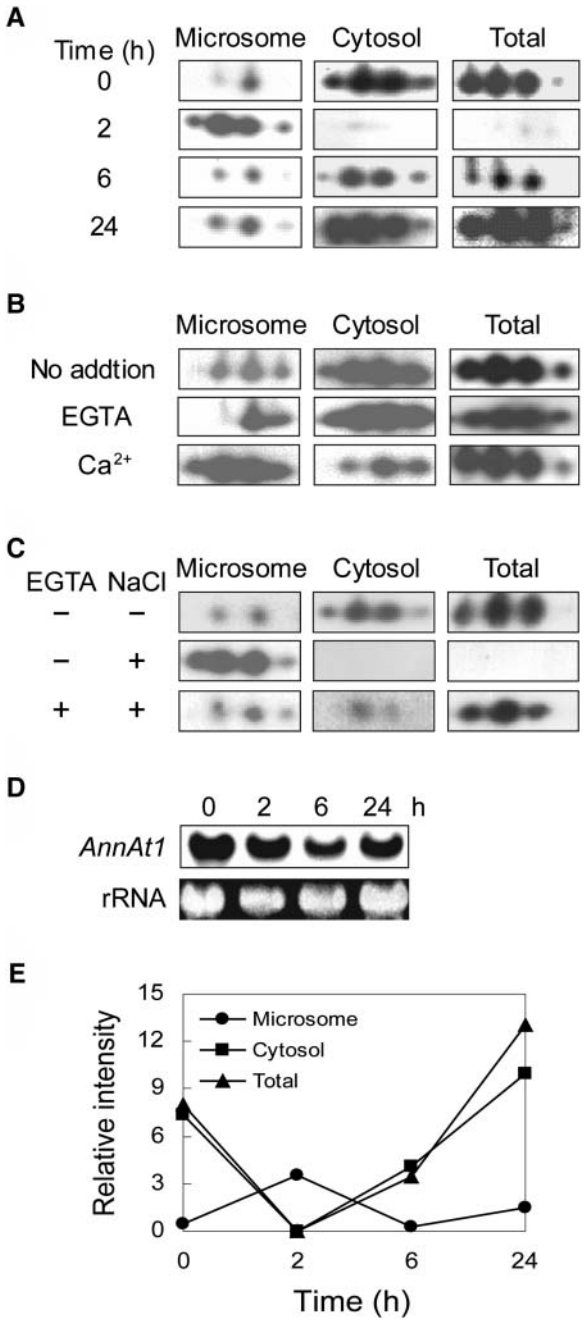

Figure 4. Salt and Calcium Response of AnnAt1 Protein.

Proteins in microsomal (microsome) and cytosolic (cytosol) fractions and the total protein extracts (total) prepared from roots of 2-week-old seedlings were subjected to 2D gel electrophoresis and protein gel blotting with the anti-AnnAt1 antibody. For the analyses, 80 μg of microsomal proteins and 40 μg of cytosolic and total proteins were used. Similar results were obtained in more than five independent experiments.

(A) AnnAt1 localization in response to NaCl. Plants were treated with 250 mM NaCl for the indicated times before harvesting.

(B) In vitro AnnAt1 localization in response to Ca^{2+}. The total protein extract was treated with either 2 mM $CaCl_2$ or 2 mM EGTA for 15 min before fractionation into the microsome and cytosol.

plants. The results strongly suggest that the salt response of AnnAt1 protein is mediated by Ca^{2+}.

We investigated whether the salt response of AnnAt1 protein is observed at the transcript level. The 3′-untranslated region (UTR) of *AnnAt1* that is specific to *AnnAt1* in RNA gel blot experiments (Clark et al., 2001) was used as a probe. RNA gel blot analysis revealed that in contrast with the salt-induced changes in protein, the transcript was not affected (Figure 4D). The *AnnAt1* level even slightly decreased over time. The data suggest that AnnAt1 is regulated translationally (i.e., by the rate of protein synthesis) or posttranslationally (i.e., by the translocation and turnover of protein).

Isolation of *AnnAt* T-DNA Insertion Mutants

To determine the in vivo function of AnnAt1, we searched the Salk Institute insertion sequence database for *annAt1* T-DNA insertion mutants. We obtained an *annAt1* mutant as well as *annAt2* and *annAt4*, other mutants of annexin family members. For *annAt2* and *annAt4*, two and three different alleles were isolated, respectively (Figure 5A). According to the data provided by the Salk Institute Genome Analysis Laboratory, the insertion positions are as follows. The *annAt1* mutant contains the T-DNA insert in the third exon, whereas the two *annAt2* alleles (*annAt2-1* and *annAt2-2*) contain the insert in the fifth exon. In the three *annAt4* mutants, T-DNA is present in the sixth exon (*annAt4-1* and *annAt4-2*) and in the 5′-UTR (*annAt4-3*). RNA analyses revealed that in some isolated mutants, the expression of each corresponding *annAt* gene was almost completely suppressed compared with the wild type (Figure 5B), which was additionally verified by protein gel blot analysis in the case of *annAt1* (Figure 5C).

To determine the exact positions of T-DNA insertions, genomic DNA fragments of *AnnAt* and T-DNA junctions were amplified and sequenced for *annAt1*, *annAt2*, and *annAt4* mutants (Figure 5A). The insertions were detected at positions of nucleotides 1192, 1605, 1670, and 1641 in *annAt1*, *annAt2-1*, *annAt4-1*, and *annAt4-2*, respectively. Furthermore, DNA gel blot analyses revealed that a single insertion is present in these lines (data not shown). In the phenotypic analyses, two independent *annAt4* alleles, *annAt4-1* and *annAt4-2*, displayed similar mutant phenotypes (Figures 6D, 7, and 8B), suggesting that a T-DNA insertion into the *AnnAt4* gene is responsible for the observed phenotypes. For *annAt1*, a genetic complementation test was additionally performed. Transformation of the mutant plant with

(C) In vivo AnnAt1 localization in response to Ca^{2+}. Plants left untreated (–) or treated (+) with 10 mM EGTA for 30 min were further incubated with (+) or without (–) 250 mM NaCl for 2 h.

(D) RNA gel blot analysis of *AnnAt1* expression in response to NaCl. Each lane was loaded with 30 μg of total RNA extracted from plants treated with 250 mM NaCl for the indicated times. Ethidium bromide–stained rRNA served as a loading control.

(E) Quantitative analysis of the data in **(A)**. The intensity of spots was assessed by densitometric measurement.

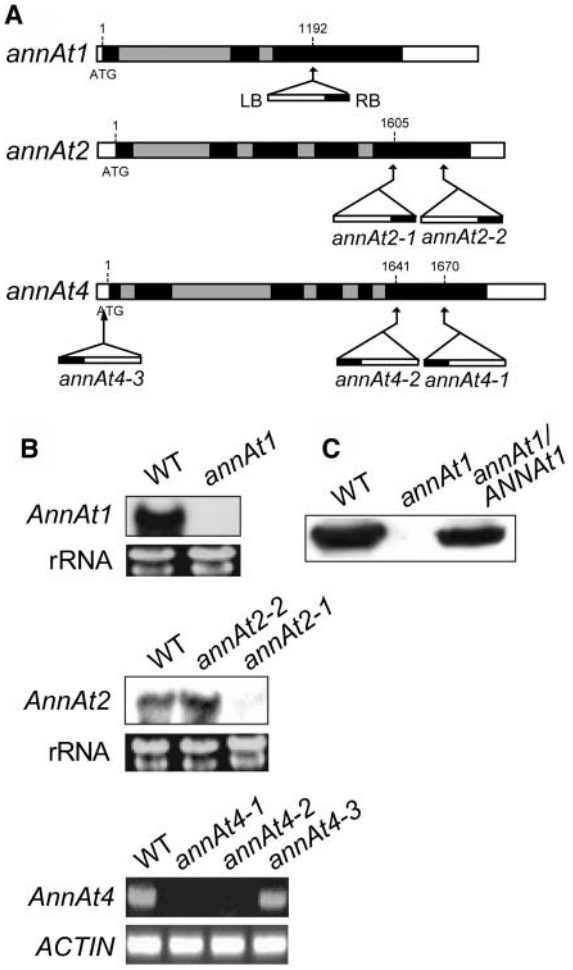

Figure 5. T-DNA Insertion Mutants of *AnnAt* Genes.

(A) Scheme of *AnnAt* genes. The arrows indicate the positions of the T-DNA insertions (triangle) within the *AnnAt1*, *AnnAt2*, and *AnnAt4* alleles. Genomic *AnnAt* DNA sequences are represented by exons (black), introns (gray), and UTRs (white). The T-DNA orientation is indicated by left (LB) and right (RB) borders. Numbers refer to nucleotides in *AnnAt* genes.

(B) RNA analysis of *AnnAt* gene expression in wild-type, *annAt1*, *annAt2*, and *annAt4* plants. *AnnAt* expression was analyzed by RNA gel blot analysis for *AnnAt1* and *AnnAt2* or RT-PCR for *AnnAt4*. For RNA gel blotting, each lane was loaded with 30 μg of total RNA extracted from wild-type, *annAt1*, and *annAt2* plants. Ethidium bromide–stained rRNA served as a loading control. RT-PCR was performed with 0.4 and 0.1 μg of total RNA for detecting *AnnAt4* and *Actin* (loading control), respectively.

(C) Protein gel blot analysis of AnnAt1 expression in wild-type, *annAt1*, and *annAt1/ANNAt1* plants. Crude extracts from root tissue were separated by SDS gel electrophoresis and subjected to protein gel blot analysis with the anti-AnnAt1 antibody.

the vector containing *AnnAt1* cDNA under the control of the 35S promoter of *Cauliflower mosaic virus* rescued the phenotypes (Figures 6F, 7E, and 8E). These plants (*annAt1/ANNAt1*) contained similar levels of AnnAt1, compared with the wild-type plants under normal growth conditions (Figure 5C). The results collectively demonstrate that T-DNA insertions provided knockout alleles of *AnnAt1* and *AnnAt4* genes.

Sensitivity of *annAt* T-DNA Insertion Mutants to NaCl

To assess the function of annexins in abiotic stress signaling, we determined the sensitivity of seed germination of *annAt* mutants to NaCl. The *annAt1*, *annAt2*, and *annAt4* mutants were allowed to germinate in media containing various concentrations of NaCl. In MS media, *annAt1* displayed slightly decreased germination, with a rate of 85% (Figure 6A). The *annAt2-1* and *annAt4-1* mutants germinated normally, similar to the wild type. Whereas only half the *annAt1* seeds germinated in the presence of 50 mM NaCl, *annAt4-1* germination was just delayed, with levels comparable to that of the wild type at 4 d after treatment (Figure 6B). However, *annAt1* and *annAt4-1* mutant seeds displayed more severely defective germination at 75 mM NaCl than the wild type and *annAt2-1* (Figure 6C). The *annAt2-1* mutant displayed similar germination patterns to the wild type at all concentrations of salt examined and sometimes rather slightly increased resistance (Figures 6B to 6D). AnnAt2 appears to play different roles in other than salt response, in contrast with AnnAt1 and AnnAt4. No significant differences were detected between *annAt4-1* and *annAt4-2* with respect to salt response (Figure 6D).

Although both *annAt1* and *annAt4* displayed hypersensitivity to NaCl, slightly different patterns were obtained in response to salt. Unlike *annAt1*, *annAt4-1* and *annAt4-2* displayed a sudden decrease in germination at 75 mM NaCl (Figure 6D). As shown in Figure 6E, seed germination of *annAt1* and *annAt4-1* was significantly affected (80% inhibition) in MS media containing 75 mM NaCl. The growth of germinated *annAt1* and *annAt4-1* plants was arrested after radicles emerged and resumed upon transfer to MS media. The results collectively suggest that AnnAt1 and AnnAt4 are implicated in salt stress response in plants.

Sensitivity of *annAt1* and *annAt4* to General Osmotic Stress

To determine whether the salt response of *annAt1* and *annAt4* results from an ionic effect, an osmotic effect, or both, germination was examined in the presence of several different ions, including KCl, LiCl, and CsCl, and mannitol as an osmotic reagent. Both *annAt1* and *annAt4* plants were sensitive to mannitol, although *annAt4* was less sensitive, similar to data observed with NaCl (Figure 7A). Interestingly, *annAt1* displayed defective germination in the presence of KCl and CsCl but was less sensitive to LiCl. By contrast, *annAt4-1* and *annAt4-2* were sensitive to LiCl and CsCl but less to KCl (Figures 7B to 7D). The results imply that *annAt1* and *annAt4* are affected by general osmotic stress and partially in an ion-specific manner, as suggested by their differential ionic specificity.

Sensitivity of *annAt1* and *annAt4* to ABA

Earlier studies suggest that ABA mediates drought and salt stress response (Leung and Giraudat, 1998; Shinozaki and Yamaguchi-Shinozaki, 2000). To test this, we investigated the germination of *annAt1* and *annAt4* mutant plants in media containing various concentrations of ABA. Both *annAt1* and

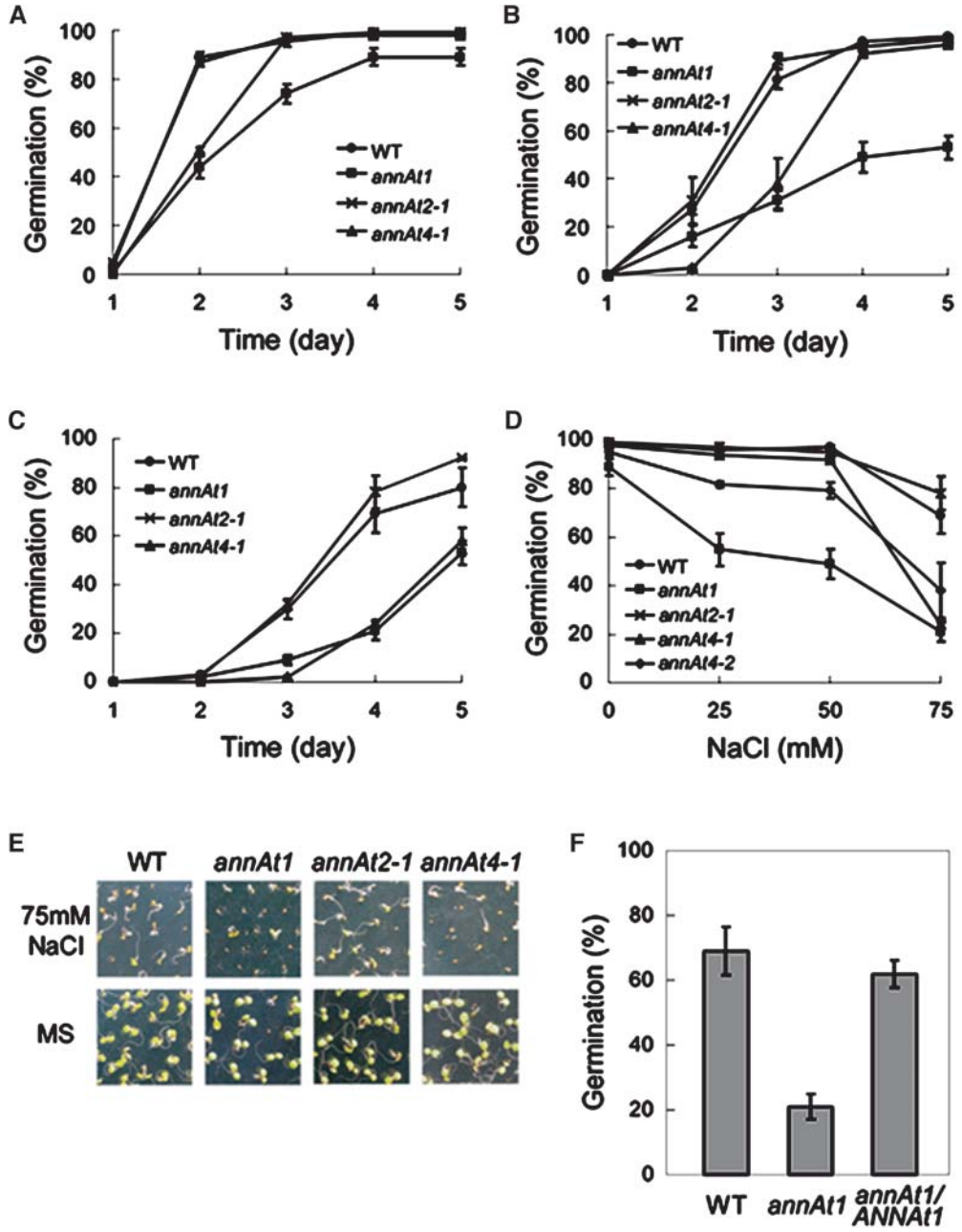

Figure 6. Sensitivity of *annAt* Mutant Plants to NaCl.

Seeds of wild-type and *annAt* mutants were plated on MS media alone or supplemented with various concentrations of NaCl after 3 d of cold treatment. The percentage of germinated seeds was determined at various times. Each data point represents the mean and standard deviation of experiments performed at least in triplicate ($n \geq 100$ each).

(A) Germination rates of wild-type and *annAt* mutants on MS media.

(B) Germination rates of wild-type and *annAt* mutants on MS media containing 50 mM NaCl.

(C) Germination rates of wild-type and *annAt* mutants on MS media containing 75 mM NaCl.

(D) NaCl dose response of germination. The germination of seeds was evaluated on MS media supplemented with the indicated concentrations of NaCl at 4 d after plating.

(E) The effect of NaCl on germination. Seeds of wild-type and *annAt* mutants were plated on MS media alone or supplemented with 75 mM NaCl and allowed to germinate for 4 d. Photographs are representative of at least five independent experiments.

(F) Complementation of the *annAt1* mutant. Analyses of wild-type, *annAt1*, and complementation transgenic lines (*annAt1*/*ANNAt1*) were performed in the presence of 75 mM NaCl as in **(E)**. Three independent complementation lines were analyzed, with similar results.

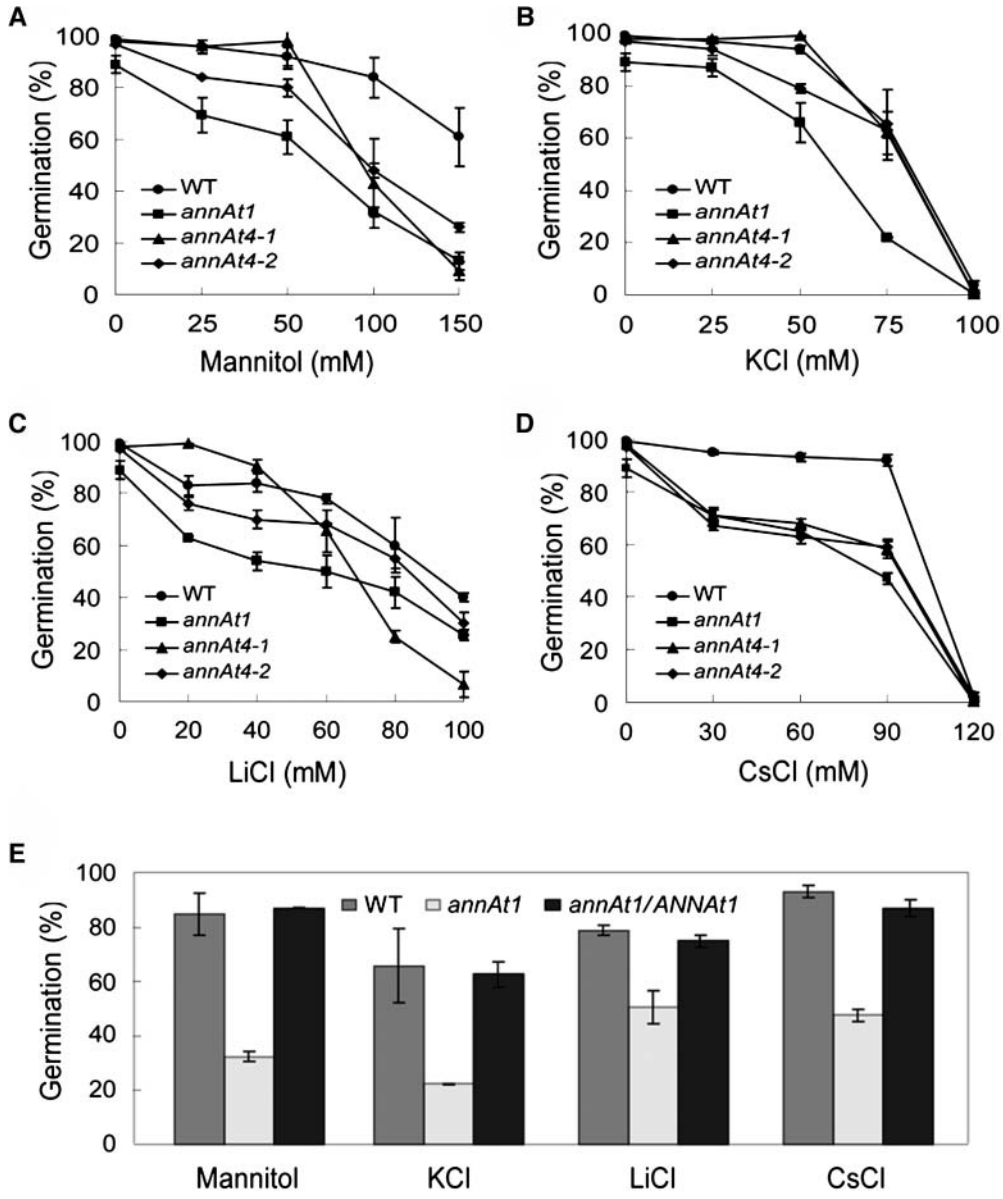

Figure 7. Sensitivity of *annAt1* and *annAt4* Mutant Plants to Osmotic Stress.

Seeds of wild-type and *annAt* mutants were plated on MS media alone or supplemented with various concentrations of mannitol and salts. The percentage of germinated seeds was determined at 4 d after plating. Each data point represents the mean and standard deviation of experiments performed at least in triplicate ($n \geq 100$ each).

(A) Mannitol dose response of germination.

(B) KCl dose response of germination.

(C) LiCl dose response of germination.

(D) CsCl dose response of germination.

(E) Complementation of the *annAt1* mutant. Analyses of wild-type, *annAt1*, and complementation transgenic lines (*annAt1/ANNAt1*) were performed in the presence of mannitol (100 mM), KCl (75 mM), LiCl (60 mM), and CsCl (90 mM). Three independent complementation lines were analyzed, with similar results.

annAt4 exhibited defective germination in the presence of ABA (Figure 8). In general, *annAt1* was more sensitive than *annAt4-1* and *annAt4-2*, particularly at lower concentrations of ABA (Figure 8B). This result is consistent with data obtained from NaCl treatment (Figure 6).

Germination of *annAt1* and *annAt4-1* plants is inhibited in media containing ABA compared with the wild type and *abi1*, the ABA-insensitive mutant line (Koornneef et al., 1984) (Figure 8C). Moreover, growth of *annAt1* and *annAt4-1* plants was impaired after radicles emerged, whereas wild-type plants continued to

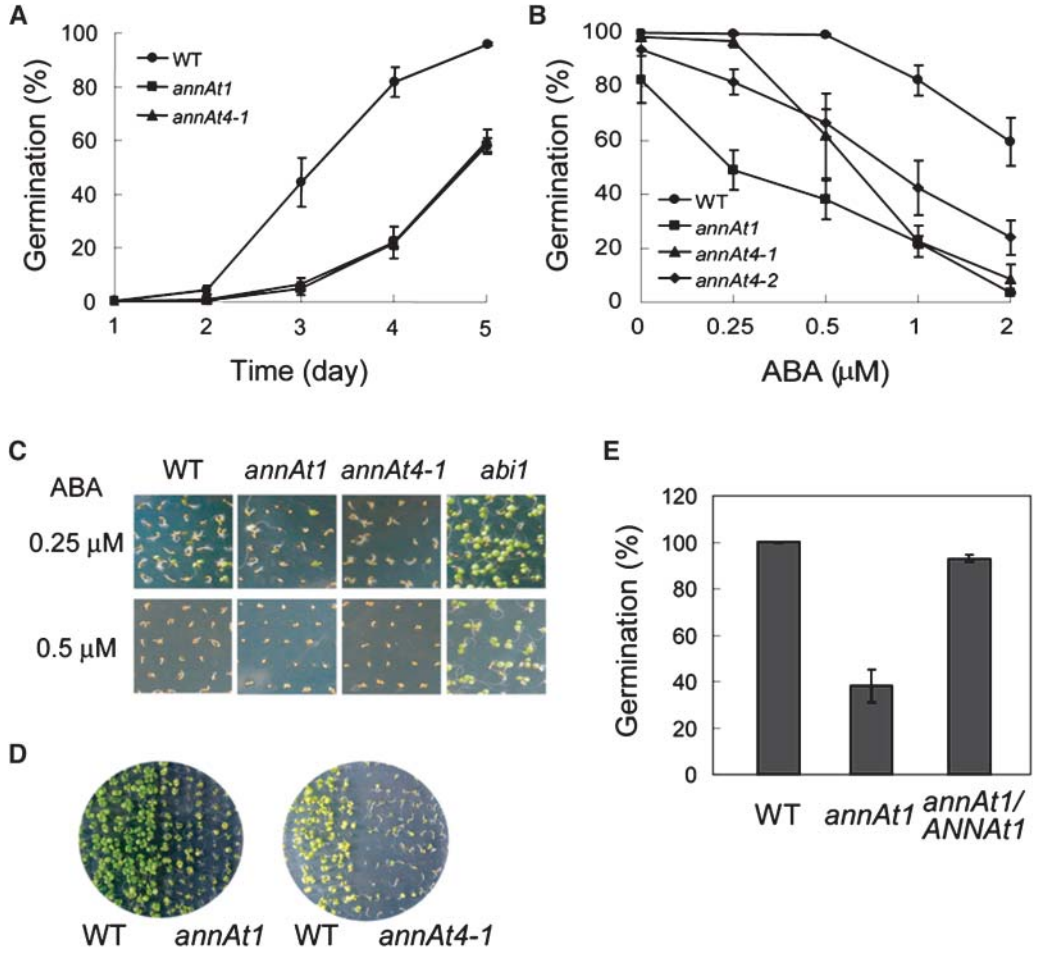

Figure 8. Sensitivity of *annAt1* and *annAt4* Mutant Plants to ABA.

(A) Germination rates of wild-type and *annAt* mutants on MS media containing 0.5 μM ABA. The percentage of germinated seeds was determined at the indicated times.

(B) ABA dose response of germination. The germination of seeds was measured on MS media supplemented with the indicated concentrations of ABA at 4 d after plating.

(C) The effect of ABA on germination. Seeds of wild-type, *abi1*, and *annAt* mutants were plated on MS media containing 0.25 and 0.5 μM ABA and allowed to germinate for 4 d.

(D) The effect of ABA on early seedling growth. Seeds of wild-type and *annAt* mutants were germinated and grown on MS media containing 0.25 μM ABA for 7 d.

(E) Complementation of the *annAt1* mutant. Analyses for wild-type, *annAt1*, and complementation transgenic lines (*annAt1/ANNAt1*) were performed in the presence of 0.5 μM ABA as in **(C)**. Three independent complementation lines were analyzed with similar results.

Data from **(A)**, **(B)**, and **(E)** are presented as the mean and standard deviation of experiments performed at least in triplicate ($n \geq 100$ each).

grow and get green (Figure 8D). We also found that *annAt1* and *annAt4-1* were in a state of growth arrest in the presence of ABA and resumed normal growth upon transfer to ABA-deficient MS media, as observed with NaCl.

DISCUSSION

Identification of AnnAt1 in the Root Microsomal Proteome

Membrane proteins play important roles in various cellular processes, modulating diverse signaling pathways. Many signals are initially perceived and transduced through active molecules located in the membrane, which regulate cell–cell interactions and responses to the environment. Therefore, we targeted the microsomal proteome containing active proteins, such as receptors, channels, and membrane-associated signaling molecules, for analysis. In this study, proteomic analyses led to the identification of the AnnAt1 protein. Levels of AnnAt1 increased upon NaCl treatment in the root microsomal proteome from Arabidopsis. Annexins are a family of Ca^{2+}-dependent membrane binding proteins that exist in nearly all species, from fungi to human (Gerke and Moss, 2002). Annexins have been

extensively studied in animal cells. These proteins are multifunctional and play important roles in various cellular processes, including membrane trafficking and organization, regulation of ion channel activity, phospholipid metabolism, inflammatory response, and mitotic signaling (Raynal and Pollard, 1994).

Expression of AnnAt1

Our results demonstrate that the 40-kD AnnAt1 protein is specifically expressed in roots, as determined by protein gel blot analysis. There were also higher molecular weight cross-reactive bands in stem and leaf tissues, which may represent multimeric forms of AnnAt1. This expression pattern is distinct from previous reports showing that *AnnAt1* is expressed in most tissues, with the highest levels either in stems or roots (Clark et al., 2001). These differences may be because of the different developmental stages or growth conditions of the plants under investigation.

Although AnnAt1 is associated with microsomes, the protein is more abundant in the cytosol. The microsomal fraction comprises membranes originating from different organelles, such as vacuole, chloroplast, Golgi, and plasma membrane. Previous reports indicate that annexins are subcellularly localized in the plasma membrane, vacuole, and nuclear periphery (Clark and Roux, 1995). To confirm subcellular localization, green fluorescent protein–fused AnnAt1 was transiently expressed in BY-2 protoplasts. AnnAt1 was detected in both the cytosol and plasma membrane, and the green fluorescent protein signal was enhanced in the plasma membrane upon salt and ABA treatment (data not shown).

Changes in AnnAt1 Protein Levels

AnnAt1 RNA expression was not affected, but protein levels were significantly altered upon the addition of NaCl into the medium, implying that the protein is subjected to translational and/or posttranslational regulation. Within 2 h of salt treatment, AnnAt1 protein levels were considerably increased in the membrane and concurrently diminished in the cytosol. This salt-induced subcellular change was accompanied by a net decrease in total AnnAt1 protein, which correlates with the finding that the major fraction of AnnAt1 exists in the cytosol. These results indicate that salt stress induces dynamic changes in AnnAt1 protein (i.e., subcellular redistribution and potential turnover of existing protein).

In many signaling processes, regulatory proteins are recruited from the cytosol to the membrane (Didichenko et al., 1996; Park et al., 2000; Oancea et al., 2003). Membrane association is often triggered by posttranslational modifications, such as phosphorylation, lipidation and glycosylation, and/or protein–protein interactions (Iwata et al., 1998). AnnAt1 was observed as at least four spots with different pI values on a 2D gel, suggesting posttranslational modifications. We are currently investigating the possibility of phosphorylation and other modifications of AnnAt1 protein, as evidenced in animal cells (Gerke and Moss, 2002). However, after stress treatment, AnnAt1 spots moved to the membrane together, implying that the possible modifications are not directly related to membrane association and play no functional roles. AnnAt1 spots remaining in the cytosol were indistinguishable from those in the membrane, supporting this finding. The formation of the cluster spots on a 2D gel may be simply because of unknown technical reasons. It is possible that the Ca^{2+}-dependent association of AnnAt1 with the membrane could also involve protein–protein interactions. Our preliminary data show that the sizes of the AnnAt1-associated complexes on a native gel differ depending on whether the complexes are isolated from the cytosolic or membrane fraction and on whether the plants are exposed to stress stimuli (data not shown). Therefore, identification of the interacting components in AnnAt1 complexes should facilitate elucidation of the specific functions of the protein and the functional significance of membrane association in stress responses. With regard to protein turnover, proteolysis, particularly the ubiquitin/26S proteasome pathway, is one of the most important regulatory mechanisms controlling cellular functions in plants (Vierstra, 2003). Several known signaling components, including phyA, HY5/HYH, AUX/IAA, NAC1, E2F, and ABI5, have been identified as target substrates. A previous report shows that annexins may be regulated by proteolysis, possibly through the lysosomal pathway, in rat lung tissue (Barnes and Gomes, 2002). Whether AnnAt1 is a selective target for the ubiquitin/26S proteasome or other proteolytic pathways would be an intriguing question.

Annexins are characterized by their ability to bind phospholipids in a Ca^{2+}-dependent manner. In this study, we provide evidence that Ca^{2+} mediates the association of AnnAt1 protein with the membrane. The inclusion of Ca^{2+} in plant extracts induced binding of AnnAt1 to the membrane, which was reversed by the addition of EGTA. In plants incubated in Ca^{2+}-chelated media, AnnAt1 lost the ability to respond to salt stress because both accumulation in the membrane and loss in the cytosol were inhibited. However, the inhibition of AnnAt1 loss from the cytoplasmic fraction was only partial. We suspect that EGTA in the media was not fully effective in chelating the intracellular Ca^{2+} that is instantly released from Ca^{2+} stores in response to stress (DeWald et al., 2001). These results imply that the salt stress–induced response of AnnAt1 is specifically regulated by Ca^{2+}. Alternatively, we cannot rule out the possibility that Ca^{2+} binding may cause conformational changes in AnnAt1 and changes in the solubility or association of this protein with other cytosolic proteins and subsequent aggregation. In addition, several fundamental questions are yet to be solved: specifically, whether the cytosolic and membrane-bound forms of AnnAt1 are structurally and functionally different and the mechanism by which Ca^{2+} induces AnnAt1 loss from the cytoplasmic fraction.

Functions of AnnAt1 and AnnAt4

The functions of annexins have been determined in a few plant species. Cotton (*Gossypium hirsutum*) fiber annexin associates with membrane callose synthase and regulates its activity (Andrawis et al., 1993). Additionally, annexin in tobacco is vacuole specific and involved in cell expansion (Seals and Randall, 1997). Several studies show that plant annexins are

highly expressed in secretory cells, such as the outer cells of root caps, epidermal cells, and developing xylem and phloem cells (Clark et al., 1992, 1994). Based on these results, it is proposed that annexins function in the Golgi-mediated secretion of plasma membrane and wall materials in plant cells (Clark and Roux, 1995). An annexin-like gene in Medicago is transcriptionally activated in response to Nod factors (de Carvalho-Niebel et al., 2002). In addition, an alfalfa annexin-like gene (*AnnMS2*) is activated by ABA, osmotic stress, and water deficiency (Kovács et al., 1998). Other functions inferred from their intrinsic activities include Ca^{2+} channel activity and enzymatic activities, such as nucleotide phosphodiesterase and peroxidase (McClung et al., 1994; Calvert et al., 1996; Gidrol et al., 1996; White et al., 2002). To date, seven annexins in Arabidopsis have been described (Clark et al., 2001). No additional *AnnAt* genes have been identified in the complete Arabidopsis genomic sequence. Among these, *AnnAt1* is induced by H_2O_2 and salicylic acid and rescues the Δ*oxyR* mutant from H_2O_2 stress when transformed into *E. coli*, suggesting a role of the protein in oxidative stress response (Gidrol et al., 1996). Despite these series of findings, further detailed studies are required to elucidate the specific functions of individual annexins in plants.

In this study, we demonstrate that AnnAt1 is possibly involved in the osmotic stress response. The *annAt1* mutant showed hypersensitivity to ABA and osmotic stress induced by such agents as NaCl, LiCl, CsCl, KCl, and mannitol in germination. In addition to *annAt1*, *annAt4* was defective in germination under stress conditions. Whereas *annAt1* and *annAt4* plants responded similarly to stress, they exhibited slightly different responses to various osmotic stress, with distinct ion selectivities and kinetics of germination. This may be because of differences in temporal and spatial expression and expression levels of proteins. AnnAt1 and AnnAt4 may have distinct, further defined roles in stress response in plants. However, we failed to detect additional altered phenotypes of *annAt1* and *annAt4* in response to ABA and osmotic stress, such as root growth inhibition and leaf wilting with growth. The data suggest that AnnAt1 and AnnAt4 may function within a restricted developmental window that includes the germination and early seedling stage. Alternatively, it is possible that the proteins exhibit functional redundancy, substituting for each other in response to stress. In contrast with *annAt1* and *annAt4*, the *annAt2* mutant exhibited normal phenotypes similar to those of the wild type in the presence of ABA and osmotic stress. Although Arabidopsis annexins are structurally conserved, their functions may be diverse and regulated in distinct ways.

At present, the mechanism by which AnnAt1 functions in ABA and osmotic stress signaling processes is unclear. It is tempting to speculate that AnnAt1 senses the Ca^{2+} signal elicited by ABA and stress and transmits it to downstream signaling pathways via dual mechanisms of protein degradation and translocation to the membrane. Degradation may release the interacting molecules, and translocation may enhance association with other molecules in the membrane, both resulting in the activation of the downstream signaling cascade. Receptors, channels, and kinases are good candidates for interacting partners. Additional studies will be required to elucidate the biological functions and action mechanisms of plant annexins.

METHODS

Plant Materials and Growth Conditions

Arabidopsis thaliana ecotype Columbia was grown in a growth room under long-day conditions (16-h-light/8-h-dark cycle). T-DNA insertion mutants, *annAt1* (SALK_015426), *annAt2-1* (SALK_054223), *annAt2-2* (SALK_054238), *annAt4-1* (SALK_019725), *annAt4-2* (SALK_039476), and *annAt4-3* (SALK_073121), were obtained from the ABRC (Columbus, OH). For plant materials, plants were either grown in soil for 3 weeks or in MS-sucrose (2%) liquid medium (Sigma, St. Louis, MO) for 2 weeks.

Germination Test

For seed germination analysis, sterilized seeds were plated on MS-sucrose (2%) agar medium. Various concentrations of NaCl, KCl, ABA, mannitol, LiCl, and CsCl were added, as described in Results. Germination (emergence of radicles) was scored daily for 5 d. Three replicate plates were used for each treatment to ensure reproducibility of data.

Complementation of the *annAt1* T-DNA Insertion Mutant

For gene complementation, the β-glucuronidase gene of the binary vector pBI121 (Clontech, Palo Alto, CA) was replaced by the *AnnAt1* coding region. The construct was transformed into *Agrobacterium tumefaciens* strain GV3101. Transformation of *annAt1* mutant plants was performed via vacuum infiltration (Bechtold and Pelletier, 1998). Transgenic plants were selected on MS plates containing kanamycin (50 μg/mL). Homozygous lines were confirmed by kanamycin resistance segregation and used for the germination test.

Preparation of Microsomal and Cytosolic Proteins

Arabidopsis seedlings were grown for 2 weeks in liquid MS medium with continuous shaking and treated with various concentrations of NaCl, ABA, PEG, and mannitol for the indicated times. Roots were harvested, immediately frozen, and ground in liquid nitrogen. The ground root powder was incubated in extraction buffer (50 mM Tris, pH 8.0, 2 mM EDTA, 2 mM DTT, 0.25 M sucrose, and protease inhibitor cocktail) and subjected to centrifugation at 8000*g* for 15 min. The supernatant (total protein extract) was then centrifuged at 100,000*g* for 1 h. After centrifugation, the supernatant (cytosolic fraction) was recovered, and the pellet (microsomal fraction) was rewashed with extraction buffer by centrifuging further at 100,000*g* for 1 h and dissolved in an appropriate volume of extraction buffer. Isolated cytosolic and microsomal fractions were divided into aliquots and either used immediately or frozen at −80°C. For protein gel blot analysis of 2D gels, 80 μg of microsomal proteins and 40 μg of cytosolic and total proteins were used.

Two-Dimensional Gel Electrophoresis

To remove lipids that interfere with isoelectric focusing, 200 μg of microsomal proteins in 200 μL were extracted with the same volume of TE (10 mM Tris, pH 8.0, and 1 mM EDTA)–saturated phenol. After centrifugation at 12,000*g* for 10 min, the upper aqueous phase was removed without disturbing the interface. The lower phase, including interface, was reextracted with two volumes of cold phenol-saturated TE buffer. After centrifugation, the upper phase was removed and proteins were precipitated with five volumes of 0.1 M ammonium acetate in methanol. Precipitated proteins were washed three times with 0.1 M ammonium acetate in methanol and once with 80% acetone.

The pellet was dried and dissolved in isoelectric focusing sample buffer (7 M urea, 2 M thiourea, 0.05% dodecylmaltoside, 4% 3-[(3-cholamidopropyl)-dimethylammonio]-1-propane sulfonate, 20 mM Tris, 20 mM

DTT, 0.5% IPG buffer, and 0.001% bromophenol blue). Immobiline DryStrips (pH 4 to 7, linear; 70 mm for protein gel blotting and 180 mm for MALDI-TOF MS analysis) (Amersham Biosciences, Uppsala, Sweden) were rehydrated with proteins and focused on the IPGphor system (Amersham Biosciences). Strips were transferred to equilibration buffer (50 mM Tris, pH 8.8, 6 M urea, 30% glycerol, 2% SDS, and 20 mM tributylphosphine [TBP]) and incubated for 15 min. When TBP is used as the reducing agent, a single step equilibration takes place using TBP and acrylamide, and iodoacetamide is not needed. The advantage of alkylating with acrylamide is to form a single alkylated product. Equilibrated strips were placed on top of vertical polyacrylaminde gels and overlaid with 0.5% agarose in SDS running buffer. After electrophoresis, 2D gels were stained with silver nitrate according to the manufacturer's manual (Amersham Biosciences). Molecular weight (MBI Fermentas, Vilnius, Lithuania) and pI (Amersham Biosciences) markers were used to calculate apparent molecular masses and pI values of spots. Two-dimensional gels were scanned and analyzed by ImageMaster 2D Elite software (Amersham Biosciences). For each condition analyzed, three to five gels were prepared from three different protein extractions. The volumes of silver-stained spots were normalized to the volumes of internal standards (e.g., spot numbers 20 and 24). The salt-induced change was subjected to statistical analysis with Student's *t* test, and those spots with $P < 0.05$ were considered for identification by MALDI-TOF MS.

Sample Preparation for MALDI-TOF MS

Peptide samples were prepared as described previously (Jensen et al., 1999). Protein spots were excised from the gel, reduced, alkylated, and digested with trypsin. Tryptic-digested peptides were recovered through a series of extraction steps. Extraction with 25 mM ammonium bicarbonate and acetonitrile was followed by second extraction step with 5% trifluoroacetic acid and acetonitrile. Extracts were pooled and lyophilized in a vacuum lyophilizer. Lyophilized tryptic peptides were redissolved in solution containing water, acetonitrile, and trifluoroacetic acid (93:5:2) and bath sonicated for 5 min. The peptide extract was prepared using the solution-phase nitrocellulose method (Landry et al., 2000).

MALDI-TOF MS and Database Searching

Peptide masses were measured on a MALDI-TOF MS (Voyager-DE STR; Perceptive Biosystems, Providence, RI) (Landry et al., 2000). Peptide mass fingerprint data were matched to the NCBI nonredundant database entries using the MS-Fit program available at the University of California San Francisco server (http://prospector.ucsf.edu/ucsfhtml4.0/msfit.htm). The following search parameters were applied. Mass tolerance was set to 50 ppm [(experimental mass−theoretical mass)/theoretical mass in daltons, parts per million], and one incomplete cleavage was allowed. Acetylation of the N terminus, alkylation of Cys by carbamidomethylation, oxidation of Met, and pyroGlu formation of N-terminal Gln were set as possible modifications. Molecular mass and pI ranges were set to 10 to 200 kD and 4 to 7, respectively. The database search disclosed matching proteins ranked according to peptide number matches, sequence coverage, and the molecular weight search (MOWSE) score. Whereas the candidate ranked at the top was considered a positive identification, protein identification was assigned when the following criteria were met: at least five matching peptides, >15% sequence coverage, and a molecular weight search score $>10^3$.

Antibody Generation and Protein Analysis

A polyclonal antibody was raised in rat to an AnnAt1-specific peptide (amino acids 204 to 215, NRYQDDHGEEIL). Immunoblotting was performed using standard protocols (Sambrook and Russell, 2001). Proteins were separated on 12% SDS-polyacrylamide gels, transferred onto nitrocellulose membranes, and incubated with the anti-AnnAt1 antibody overnight at 4°C. Antibody-bound proteins were detected after incubation with secondary antibody conjugated to horseradish peroxidase using the ECL system (Amersham Biosciences). For fair comparison of gels, sets of blots incorporated in a figure were simultaneously processed for protein gel blot analysis under the same conditions.

RNA Analysis

RNA was isolated using the TRI reagent (MRC, Cincinnati, OH) according to the manufacturer's instructions. For RNA gel blot analysis, 30 μg of total RNA was fractionated on a 1.2% formaldehyde-agarose gel, transferred to a nylon membrane (Hybond N+; Amersham Biosciences) and fixed using the UV cross-linker (Stratagene, La Jolla, CA). Loading of equal amounts of RNA was confirmed by ethidium bromide staining. The gene-specific 3′-UTR probes were amplified by PCR using the following primers: for *AnnAt1*, 5′-GCTTAATCAATCAATCCTCC-3′ and 5′-CTCAAAACACACAACAGAAAC-3′; for *AnnAt2*, 5′-GCGATGCTTGAAACTGTTTC-3′ and 5′-CAAACTCAAACGATCATTGAT-3′. Hybridization was performed in Rapid-Hyb buffer (Amersham Biosciences) for 16 to 24 h at 65°C. After hybridization, membranes were serially washed in 2× SSC (1× SSC is 0.15 M NaCl and 0.015 M sodium citrate)/0.1% SDS, 1× SSC/0.1% SDS, and finally 0.1% SSC/0.1% SDS. RNA bands were visualized by autoradiography.

RT-PCR was performed with 0.4 and 0.1 μg of total RNA for the detection of *AnnAt4* and *Actin*, respectively, using the Access RT-PCR system (Promega, Madison, WI). The primers used to amplify the cDNA fragments were as follows: *AnnAt4*, 5′-ACACTGGGGAAATCGCAAAAG-3′ and 5′-AGCCAAAGTCTCACCATAAAG-3′; *Actin*, 5′-GGCGATGAAGCTCAATCCAAACG-3′ and 5′-GGTCACGACCAGCAAGATCAAGACG-3′. The primers produced 801-bp and 491-bp products for *AnnAt4* and *Actin*, respectively.

Sequence data from this article have been deposited with the GenBank/EMBL data libraries under the following accession numbers: *AnnAt1* (At1g35720), *AnnAt2* (At5g65020), and *AnnAt4* (At2g38750).

ACKNOWLEDGMENTS

We are grateful to Moon Soo Soh for technical comments. We also thank Mi-Ok Han for technical assistance. This research was supported by grants from the Crop Functional Genomics Center of 21st Century Frontier Research Program funded by the Ministry of Science and Technology (M101KG010001-03K0701-01620) and the Plant Signaling Network Research Center funded by the Korea Science and Engineering Foundation. This article is Kumho Life and Environmental Science Laboratory publication number 66.

Received February 10, 2004; accepted March 8, 2004.

REFERENCES

Andrawis, A., Solomon, M., and Delmer, D.P. (1993). Cotton fiber annexins: A potential role in the regulation of callose synthase. Plant J. **3,** 763–772.

Barnes, J.A., and Gomes, A.V. (2002). Proteolytic signals in the primary structure of annexins. Mol. Cell. Biochem. **231,** 1–7.

Bechtold, N., and Pelletier, G. (1998). In planta *Agrobacterium*-mediated transformation of adult *Arabidopsis thaliana* plants by vacuum infiltration. Methods Mol. Biol. **82,** 259–266.

Calvert, C.M., Gant, S.J., and Bowles, D.J. (1996). Tomato annexins p34 and p35 bind to F-actin and display nucleotide phosphodiesterase activity inhibited by phospholipid binding. Plant Cell **8,** 333–342.

Clark, G.B., Dauwalder, M., and Roux, S.J. (1992). Purification and immunolocalization of an annexin-like protein in pea seedlings. Planta **187,** 1–9.

Clark, G.B., Dauwalder, M., and Roux, S.J. (1994). Immunolocalization of an annexin-like protein in corn. Adv. Space Res. **14,** 341–346.

Clark, G.B., and Roux, S.J. (1995). Annexins of plant cells. Plant Physiol. **109,** 1133–1139.

Clark, G.B., Sessions, A., Eastburn, D.J., and Roux, S.J. (2001). Differential expression of members of the annexin multigene family in Arabidopsis. Plant Physiol. **126,** 1072–1084.

Davies, W.J., and Zhang, J.H. (1991). Root signals and the regulation of growth and development of plants in drying soil. Annu. Rev. Plant Physiol. Plant Mol. Biol. **42,** 55–76.

de Carvalho-Niebel, F., Timmers, A.C.J., Chabaud, M., Defaux-Petrae, A., and Barker, D.G. (2002). The Nod-factor-elicited annexin MtAnn1 is preferentially localized at the nuclear periphery in symbiotically activated root tissues of *Medicago truncatula*. Plant J. **32,** 343–352.

DeWald, D.B., Torabinejad, J., Jones, C.A., Shope, J.C., Cangelosi, A.R., Thompson, J.E., Prestwich, G.D., and Hama, M. (2001). Rapid accumulation of phosphatidylinositol 4,5-bisphosphate and inositol 1,4,5-trisphosphate correlates with calcium mobilization in salt-stressed Arabidopsis. Plant Physiol. **126,** 759–769.

Didichenko, S.A., Tilton, B., Hemmings, B.A., Ballmer-Hofer, K., and Thelen, M. (1996). Constitutive activation of protein kinase B and phosphorylation of p47phox by a membrane-targeted phosphoinositide 3-kinase. Curr. Biol. **6,** 1271–1278.

Dove, S.K., Cooke, F.T., and Michell, R.H. (1997). Osmotic stress activates phosphatidylinositol-3,5-bisphosphate synthesis. Nature **390,** 187–192.

Droillard, M., Boudsocq, M., Barbier-Brygoo, H., and Lauriere, C. (2002). Different protein kinase families are activated by osmotic stresses in *Arabidopsis thaliana* cell suspensions. Involvement of the MAP kinases AtMPK3 and AtMPK6. FEBS Lett. **527,** 43–50.

Gerke, V., and Moss, S.E. (2002). Annexins: From structure to function. Physiol. Rev. **82,** 331–371.

Gidrol, X., Sabelli, P.A., Fern, Y.S., and Kush, A.K. (1996). Annexin-like protein from *Arabidopsis thaliana* rescues Δ*oxyR* mutant of *Escherichia coli* from H_2O_2 stress. Proc. Natl. Acad. Sci. USA **93,** 11268–11273.

Giraudat, J., Parcy, F., Bertauche, N., Gosti, F., and Leung, J. (1994). Current advances in abscisic acid action and signaling. Plant Mol. Biol. **26,** 1557–1577.

Halfter, U., Ishitani, M., and Zhu, J.-K. (2000). The Arabidopsis SOS2 protein kinase physically interacts with and is activated by the calcium-binding protein SOS3. Proc. Natl. Acad. Sci. USA **97,** 3735–3740.

Harmon, A.C., Gribskov, M., and Harper, J.F. (2000). CDPKs: A kinase for every Ca^{2+} signal? Trends Plant Sci. **5,** 154–159.

Himmelbach, A., Yang, Y., and Grill, E. (2003). Relay and control of abscisic acid signaling. Curr. Opin. Plant Biol. **6,** 470–479.

Ichimura, K., Mizoguchi, T., Yoshida, R., Yuasa, T., and Shinozaki, K. (2000). Various abiotic stresses rapidly activate Arabidopsis MAP kinases ATMPK4 and ATMPK6. Plant J. **24,** 655–665.

Iwata, S., Lee, J.W., Okada, K., Lee, J.K., Iwata, M., Rasmussen, B., Link, T.A., Ranaswamy, S., and Jap, B.K. (1998). Complete structure of the 11-subunit bovine mitochondrial cytochrome bc1 complex. Science **281,** 64–71.

Jensen, O.N., Wilm, M., Shevchenko, A., and Mann, M. (1999). Sample preparation methods for mass spectrometric peptide mapping directly from 2-DE gels. Methods Mol. Biol. **112,** 513–530.

Kiegle, E., Moore, C.A., Haseloff, J., Tester, M.A., and Knight, M.R. (2000). Cell-type-specific calcium responses to drought, salt and cold in the Arabidopsis root. Plant J. **23,** 267–278.

Knight, H., and Knight, M.R. (2001). Abiotic stress signaling pathways: Specificity and cross-talk. Trends Plant Sci. **6,** 262–267.

Knight, H., Trewavas, A.J., and Knight, M.R. (1996). Cold calcium signaling in Arabidopsis involves two cellular pools and a change in calcium signature after acclimation. Plant Cell **8,** 489–503.

Knight, H., Trewavas, A.J., and Knight, M.R. (1997). Calcium signalling in *Arabidopsis thaliana* responding to drought and salinity. Plant J. **12,** 1067–1078.

Koornneef, M., Reuling, G., and Karssen, C. (1984). The isolation and characterization of abscisic acid-insensitive mutants of *Arabidopsis thaliana*. Physiol. Plant **61,** 377–383.

Kovács, I., Ayaydin, F., Oberschall, A., Ipacs, I., Bottka, S., Ponger, S., Dudits, D., and Tóth, E.C. (1998). Immunolocalization of a novel annexin-like protein encoded by a stress and abscisic acid responsive gene in alfalfa. Plant J. **15,** 185–197.

Landry, F., Lombardo, C.R., and Smith, J.W. (2000). A method for application of samples to matrix-assisted laser desorption ionization time-of-flight targets that enhances peptide detection. Anal. Biochem. **279,** 1–8.

Leung, J., and Giraudat, J. (1998). Abscisic acid signal transduction. Annu. Rev. Plant Physiol. Plant Mol. Biol. **49,** 199–222.

Liu, J., and Zhu, J.-K. (1997). An Arabidopsis mutant that requires increased calcium for potassium nutrition and salt tolerance. Proc. Natl. Acad. Sci. USA **94,** 14960–14964.

Liu, J., and Zhu, J.-K. (1998). A calcium sensor homolog required for plant salt tolerance. Science **280,** 1943–1945.

Luan, S., Kudla, J., Rodriguez-Concepcion, M., Yalovsky, S., and Gruissem, W. (2002). Calmodulin and calcineurin B-like proteins: Calcium sensors for specific signal response coupling in plants. Plant Cell **14** (suppl.), S389–S400.

McClung, A.D., Carroll, A.D., and Battey, N.H. (1994). Identification and characterization of ATPase activity associated with maize (*Zea mays*) annexins. Biochem. J. **303,** 709–712.

Mikolajczyk, M., Olubunmi, S.A., Muszynska, G., Klessig, D.F., and Dobrowolska, G. (2000). Osmotic stress induces rapid activation of a salicylic acid-induced protein kinase and a homolog of a protein kinase ASK1 in tobacco cells. Plant Cell **12,** 165–178.

Munnik, T., Irvine, R.F., and Musgrave, A. (1999). Distinct osmosensing protein kinase pathways are involved in signaling moderate and severe hyperosmotic stress. Plant J. **20,** 381–388.

Munnik, T., Meijer, H.J., Ter Riet, B., Hirt, H., Frank, W., Bartels, D., and Musgrave, A. (2000). Hyperosmotic stress stimulates phospholipase D activity and elevates the levels of phosphatidic acid and diacylglycerol pyrophosphate. Plant J. **22,** 147–154.

Oancea, E., Bezzerides, V.J., Greka, A., and Clapham, D.E. (2003). Mechanism of persistent protein kinase D1 translocation and activation. Dev. Cell **4,** 561–574.

Park, J., Choi, H.J., Lee, S., Lee, T., Yang, Z., and Lee, Y. (2000). Rac-related GTP-binding protein in elicitor-induced reactive oxygen generation by suspension-cultured soybean cells. Plant Physiol. **124,** 725–732.

Qiu, Q.S., Guo, Y., Dietrich, M.A., Schumaker, K.S., and Zhu, J.-K. (2002). Regulation of SOS1, a plasma membrane Na^+/H^+ exchanger in *Arabidopsis thaliana*, by SOS2 and SOS3. Proc. Natl. Acad. Sci. USA **99,** 8436–8441.

Quintero, F.J., Ohta, M., Shi, H., Zhu, J.K., and Pardo, J.M. (2002). Reconstitution in yeast of the Arabidopsis SOS signaling pathway for Na^+ homeostasis. Proc. Natl. Acad. Sci. USA **99,** 9061–9066.

Raynal, P., and Pollard, H.B. (1994). Annexins: The problem of assessing the biological role for gene family of multifunctional

Ca^{2+}-and phospholipid-binding proteins. Biochem. Biophys. Acta **1197,** 63–93.

Romeis, T., Ludwig, A.A., Martin, R., and Jones, J.D. (2001). Calcium-dependent protein kinases play an essential role in a plant defence response. EMBO J. **20,** 5556–5567.

Sajio, Y., Hata, S., Kyozuka, J., Shimamoto, K., and Izui, K. (2000). Over-expression of a single Ca^{2+}-dependent protein kinase confers both cold and salt/drought tolerance on rice plants. Plant J. **23,** 319–327.

Sambrook, J., and Russell, D.W. (2001). Molecular Cloning: A Laboratory Manual, 3rd ed. (Cold Spring Harbor, NY: Cold Spring Harbor Laboratory Press).

Seals, D.F., and Randall, S.K. (1997). A vacuole-associated Annexin protein, VcaB42, correlates with the expansion of tobacco cells. Plant Physiol. **115,** 735–761.

Sheen, J. (1996). Ca^{2+} dependent protein kinases and stress signal transduction in plants. Science **274,** 1900–1902.

Shinozaki, K., and Yamaguchi-Shinozaki, K. (2000). Molecular response to dehydration and low temperature: Differences and cross-talk between two stress signaling pathways. Curr. Opin. Plant Biol. **3,** 217–223.

Skriver, K., and Mundy, J. (1990). Gene expression in response to abscisic and osmotic stress. Plant Cell **2,** 503–512.

Townely, H.E., and Knight, M.R. (2002). Calmodulin as a potential negative regulator of Arabidopsis COR gene expression. Plant Physiol. **128,** 1169–1172.

Trewavas, A. (1999). Le calcium, C'est la vie: Calcium makes waves. Plant Physiol. **120,** 1–6.

Vierstra, R.D. (2003). The ubiquitin/26S proteasome pathway, the complex last chapter in the life of many plant proteins. Trends Plant Sci. **8,** 135–142.

White, P.J., Bowen, H.C., Demidchik, V., Nichols, C., and Davies, J.M. (2002). Genes for calcium-permeable channels in the plasma membrane of plant root cells. Biochim. Biophys. Acta **1564,** 299–309.

Wu, S.J., Ding, L., and Zhu, J.-K. (1996). SOS1, a genetic locus essential for salt tolerance and potassium acquisition. Plant Cell **8,** 617–627.

Xiong, L., Schumaker, K.S., and Zhu, J.-K. (2002). Cell signaling during cold, drought, and salt stress. Plant Cell **14** (suppl.), S165–S183.

Zeevaart, J.A.D., and Creelman, R.A. (1998). Metabolism and physiology of abscisic acid. Annu. Rev. Plant Physiol. Plant Mol. Biol. **39,** 439–473.

Zhu, J.-K. (2002). Salt and drought stress signal transduction in plants. Annu. Rev. Plant Biol. **53,** 247–273.

Zhu, J.-K., Liu, J., and Xiong, L. (1998). Genetic analysis of salt tolerance in arabidopsis. Evidence for a critical role of potassium nutrition. Plant Cell **10,** 1181–1191.

Zielinski, R.E. (1998). Calmodulin and calmodulin-binding proteins in plants. Annu. Rev. Plant Physiol. Plant Mol. **49,** 697–725.